RSC Advances

PAPER

View Article Online
View Journal | View Issue

Cite this: *RSC Adv.*, 2017, **7**, 25387

Biodegradation of the neonicotinoid insecticide acetamiprid in surface water by the bacterium *Variovorax boronicumulans* CGMCC 4969 and its enzymatic mechanism†

Shi-Lei Sun,[a] Wen-Long Yang,[a] Jing-Jing Guo,[a] Yi-Ning Zhou,[a] Xue Rui,[a] Chen Chen,[a] Feng Ge*[b] and Yi-Jun Dai*[a]

Received 6th February 2017
Accepted 3rd May 2017

DOI: 10.1039/c7ra01501a

rsc.li/rsc-advances

The plant growth-promoting rhizobacterium *Variovorax boronicumulans* CGMCC 4969 was used to degrade the neonicotinoid insecticide, acetamiprid (AAP), in surface water, and the enzymatic mechanisms of AAP degradation in *V. boronicumulans* CGMCC 4969 were explored. *V. boronicumulans* CGMCC 4969 degraded 34.7% of 2 mg L^{-1} AAP over 120 h with a degradation half-life of 182 h in surface water, and the major metabolite was the amide product, (*E*)-N^2-carbamoyl-N^1-[(6-chloro-3-pridyl) methyl]-N^1-methylacetamidine (IM-1-2). Gene cloning and over-expression studies proved that AAP hydration to IM-1-2 was mediated by a nitrile hydratase (ANHase). Addition of AAP to the mineral salt medium (MSM) broth significantly upregulated the ANHase gene expression by 1.6-fold, when compared with that in the control without AAP. Co-expression of the ANHase gene with its activator gene (*anhC*) apparently increased ANHase activity 21-fold for AAP hydration compared with the ANHase gene alone. The independent over-expression of *anhC* gave rise to competitive inhibition on the β-subunit of the ANHase and resulted in decreased ANHase activity. This ANHase is versatile, hydrating aromatic, N-heterocyclic, and aliphatic nitrile compounds. The present study shows the potential of *V. boronicumulans* CGMCC 4969 in the bioremediation of AAP contaminated water.

1. Introduction

Neonicotinoids are a class of heterocyclic ring-containing systemic pesticides, which are used for the control of sucking insect pests such as aphids, whiteflies, planthoppers, thrips, some micro-Lepidoptera, and coleopteran pests.[1] They act as an agonist and selectively bind the nicotinic acetylcholine receptor in the central nervous system of the insect, leading to paralysis and death.[2] Recent studies have shown that neonicotinoid insecticides may not only affect pest insects but also non-target organisms such as pollinators and birds.[3] Because most neonicotinoids persist in soils for a year or more and are water soluble, more than 80% of neonicotinoid residues remaining in the soil of treated crops eventually enter surface waters or groundwater. Recent surveys in nine countries showed 80% of surface waters were contaminated with neonicotinoids at levels of 0.14 to 18 μg L^{-1},[4] which are sublethal to aquatic arthropods.

Among the seven commercial neonicotinoid insecticides, acetamiprid (AAP) belongs to the chloronicotinyl subclass and its widespread use is due to its high stability and insecticidal activity. However, recent studies suggested that AAP causes acute and chronic toxicity in mammals and, moreover, AAP has become the focus of attention because of its apparent toxicity to bees.[5,6] In addition, AAP is highly water soluble at 4.25 g L^{-1}, which is 20-fold higher than another neonicotinoid, thiacloprid (THI), containing the same pharmacophore cyanoguanidine moiety. Because of this AAP easily leaches into surface water and groundwater, and therefore AAP residues in aqueous environments have been detected in some recent reports. For example, Leandro *et al.* detected AAP in shallow groundwater in a cotton-growing region of Mato Grosso, Brazil.[7] Anderson *et al.* reported AAP detection in the playa wetlands of Texas.[8] Wu *et al.* detected AAP at a concentration of 0.2 μg L^{-1} in the Jingmi River, Beijing, China.[9] Struger reported that AAP was detected at concentrations greater than the guideline value in the surface waters of southern Ontario, Canada.[10] AAP also persists regardless of bio-treatment and has been found in wastewater treatment plant effluents in concentrations ranging from 50 ng L^{-1} to 16 μg L^{-1}.[11] The AAP residues in water may affect

[a]*Jiangsu Key Laboratory for Microbes and Functional Genomics, Jiangsu Engineering and Technology Research Center for Industrialization of Microbial Resources, College of Life Science, Nanjing Normal University, Nanjing 210023, People's Republic of China. E-mail: daiyijun@njnu.edu.cn; Fax: +86-25-85891067; Tel: +86-25-85891731*

[b]*Nanjing Institute of Environmental Sciences, Ministry of Environmental Protection, Nanjing 210042, People's Republic of China. E-mail: gefeng@nies.org*

† Electronic supplementary information (ESI) available. See DOI: 10.1039/c7ra01501a

the sensitive aquatic invertebrates living in it and therefore produce risks to the ecosystem.

AAP is known to be stable under alkaline conditions and can persist for more than 30 d.[12] Elimination of AAP residues from the environment by chemical and photochemical methods have been largely reported. Khan *et al.* reported heterogeneous photocatalysed degradation of AAP in aqueous suspensions of a semiconductor.[13] Mitsika *et al.* employed the Fenton reaction to oxidize AAP in water samples.[14] However, chemical degradation of AAP is expensive, environmentally harmful, and requires extreme conditions. In contrast, microbial degradation could avoid these disadvantages and is a promising approach for the remediation of AAP contamination. Many microorganisms have been reported to degrade AAP. For example, the yeast *Rhodotorula mucilaginosa* IM-2 transformed AAP to IM-1-3.[15] The bacterium *Ensifer meliloti* CGMCC 7333 degraded AAP to IM-1-2.[16] *Pigmentiphaga* sp. AAP-1 and D-2 and *Stenotrophomonas* sp. THZ-XP degraded AAP to form IM-1-4.[17–19] The bacterium *Rhodococcus* sp. BCH2 degraded AAP to IM-1-4, which was further degraded to IC-O.[20] The bacterium *Stenotrophomonas maltophilia* CGMCC 1.1788 degraded AAP *via N*-demethylation to form IM 2-1.[21] In a previous study, we reported that the plant growth-promoting rhizobacterium *Variovorax boronicumulans* CGMCC 4969 degraded thiacloprid to its amide metabolite and the carcinogen acrylamide to acrylic acid.[22,23] Bacteria belonging to the genus *Variovorax* are common inhabitants of water and soil. *Variovorax* species display diverse metabolic features and catabolic capabilities making them a promising choice for applications in bioremediation studies. For example, *V. paradoxus* was used as a bioaugmentation agent for the bioremediation of pesticide linuron-contaminated soils.[24] Because there have been no reports on AAP biodegradation in aqueous environments, we primarily investigated the ability of *V. boronicumulans* CGMCC 4969 to bioremediate AAP contamination in surface water samples. Meanwhile, the genomic DNA of *V. boronicumulans* CGMCC 4969 has been sequenced to identify the corresponding gene clusters involved in AAP degradation and these genes were functionally over-expressed in *Escherichia coli*. The characteristics of the CGMCC 4969 enzyme over-expressed in *E. coli* that was responsible for AAP degradation were studied in detail.

2. Experimental

2.1 Chemicals and media

AAP and THI were obtained from Jiangsu Pesticide Research Institute Company Ltd., Nanjing, China (>97% purity). Indole-3-acetonitrile (IAN), benzonitrile, butyronitrile, 2-cyanopyridine, 3-cyanopyridine, hexanedinitrile, isobutyronitrile, and succinonitrile were purchased from Sigma-Aldrich (Shanghai, China; each of 98% purity). HPLC grade acetonitrile and methanol were purchased from TEDIA (Fairfield, OH, USA). All other reagents were of analytical grade and purchased from Sinopharm Chemical Reagent Co., Ltd. (Shanghai, China). The broth for cell cultivation was Luria–Bertani medium containing 10.0 g of peptone, 5.0 g of yeast extract, and 10.0 g of NaCl per liter of water. MSM medium contained 1.36 g of KH_2PO_4, 2.13 g of Na_2HPO_4, 0.50 g of $MgSO_4 \cdot 7H_2O$, and 10 mL of metal solution in 1.0 L of deionized water (pH 7.5). The metal solution contained 0.40 g of $CaCl_2 \cdot 2H_2O$, 0.30 g of H_3BO_3, 0.04 g of $CuSO_4 \cdot 5H_2O$, 0.10 g of KI, 0.20 g of $FeSO_4 \cdot 7H_2O$, 0.40 g of $MnSO_4 \cdot 7H_2O$, 0.20 g of $NaMoO_4 \cdot 2H_2O$, and 10.0 mL of concentrated HCl in 1.0 L of deionized water.

2.2 Bacterial strains and plasmids

The wild bacterium *V. boronicumulans* CGMCC 4969 was deposited in the China General Microbiological Culture Collection Center (CGMCC) (Beijing, China). *Escherichia coli* Rosetta (DE3) was used as a host strain for gene over-expression and stored in our laboratory. The plasmids pET28a (+) and pET21a (+) (Novagen, Inc., Madison, WI, USA) were used as expression vectors.

2.3 Biodegradation of AAP by *V. boronicumulans* CGMCC 4969 in surface water samples

Resting cells of *V. boronicumulans* CGMCC 4969 were used for AAP degradation and their preparation was described in our previous report.[25] These resting cells were used to determine the AAP degradation in surface water samples. The water samples were collected from CaiYue Lake, Nanjing, China. The physicochemical properties of the collected water were: pH 7.0; total phosphorus of 0.08 mg L^{-1}, total Kjeldahl nitrogen of 2.24 mg L^{-1}, and chemical oxygen demand of 4.37 mg L^{-1}. The water samples were filtered through a sterilized 0.22 μm membrane. 20 mL of each water sample were poured into a 100 mL flask and then the resting cells of *V. boronicumulans* CGMCC 4969 were added to a final concentration of 1.3×10^8 cell per mL while the final AAP concentration was 2 mg L^{-1}. AAP degradation broth excluding bacterial cells was used as a control. The experiments were conducted under the above cultivation conditions. Every 24 h, 1 mL of the broth was collected and centrifuged at 12 000 *g* for 10 min to remove residual cells, and the supernatant was filtered using a 0.22 μm membrane prior to HPLC analysis.

2.4 Chemical analysis

The degradation of AAP was analyzed using an Agilent 1200 HPLC system equipped with an HC-C18 column (4.6 × 250 mm, Agilent Technologies, Santa Clara, CA, USA). The mobile phase contained water, acetonitrile, and 0.01% acetic acid (water/acetonitrile, 65 : 35). The flow rate of the mobile phase was 1 mL min^{-1}. The signal was monitored at a wavelength of 235 nm. LC-MS was conducted using an Agilent 1290 HPLC-DAD and an Agilent 6460 HPLC-q3MS/MS system equipped with an electrospray ion source (Agilent Technologies, Wilmington, DE, USA) that was operated in the positive ion mode. For the other aromatic nitriles, the HPLC conditions were the same as those in a previous report.[26] The ^1H and ^{13}C NMR spectra for the metabolite were obtained by using a Bruker AV-400 NMR spectrometer (Bruker, Faellanden, Switzerland) operating at 400 and 100 MHz, respectively. The solvent for NMR analysis was dimethylsulfoxide-d6. Chemical shifts were referenced against internal tetramethylsilane. Several NMR techniques were used

Table 1 qRT-PCR primer sets used in this study

Target genes	Primer	Sequence (5′–3′)	Amplicon size (bp)
NHase	NHa-F	GCCAATACCGACGACCAGCAC	172
	NHa-R	TGGTCTCGGGCAAGGTGGT	
16S	16S-F	TACTGGGCGTAAAGCGTGCG	174
	16S-R	ATTGCCTTCGCCATCGGTGT	

to assign proton and carbon atom chemical shifts (δ), including distortionless enhancement by polarization transfer, heteronuclear single-quantum correlation spectroscopy, and heteronuclear multiple bond correlation.

2.5 RNA extraction and quantitative PCR

2.5.1 RNA extraction. For the extraction of total RNA, the *V. boronicumulans* CGMCC 4969 cells were cultivated in MSM medium containing 2 g L^{-1} glucose, 20 mg L^{-1} AAP or 2 g L^{-1} glucose, and 2 g L^{-1} KNO_3 at 30 °C and 200 rpm, and harvested after 2 days. The total RNA was isolated using the spin-column bacterial total RNA purification kit (Sangon Biotech, Shanghai, China), following the manufacturer's instructions. The RNA concentration was calculated by measuring the absorbance at 260 nm, and the purity was evaluated based on the ratios of 260/280 nm using a Nanodrop spectrophotometer (Nanodrop Technologies, Wilmington, DE, USA).

2.5.2 Reverse transcription quantitative PCR. The extracted total RNA (1 μg) was reverse-transcribed using the PrimeScript™ RT reagent kit with gDNA Eraser (Takara Biotech, Dalian, China). The synthesized cDNA was subjected to quantitative real-time PCR (qPCR) using the Applied Biosystems Step One Real-Time PCR Systems (Carlsbad, CA, USA) and SYBR *Premix Ex Taq* II (Tli RNaseH Plus, Takara Biotech). Specific primers were designed using Primer Premier 5.0 software (Premier Biosoft International, Palo Alto, CA, USA), and are listed in Table 1. The qPCR was performed in a 20 μL mixture containing 10 μL of SYBR *Premix Ex Taq* II (Tli RNaseH Plus) (2×), 0.8 μL of each primer (10 mmol L^{-1}), 0.4 μL of ROX Reference Dye (50×), 2 μL of cDNA template, and 6 μL of sterilized distilled water. The thermal cycling conditions were as follows: 95 °C for 30 s, followed by 40 cycles at 95 °C for 5 s and 60 °C for 30 s. A melting curve was analyzed at the end of the qPCR to verify specific amplification. The 16S rRNA gene was used as a reference gene to normalize the amount of RNA in each sample. Each sample was measured in triplicate.

2.6 Construction of plasmids containing different components of the CGMCC 4969 ANHase gene cluster

A MiniBEST bacterial genomic DNA extraction kit (TaKaRa, Dalian, China) was employed for the extraction of the genomic DNA of *V. boronicumulans* CGMCC 4969. The sequence of the genomic DNA was determined by the Huada Genomics Institute (Shenzhen, China). Plasmids containing different components of the ANHase gene cluster (Fig. 1) were constructed to clarify the functions of the independent genes in the ANHase gene cluster responsible for AAP degradation. The primers are listed in Table 2 and were synthesized by Sangon Biotech (Shanghai) Co., Ltd.

To investigate the influence of the downstream hypothetical protein (ANHc) on ANHase activity, two plasmids named pNAB and pNABC containing ANHase structural genes without and with *anhC* were constructed, respectively (Fig. 1). The ANHase

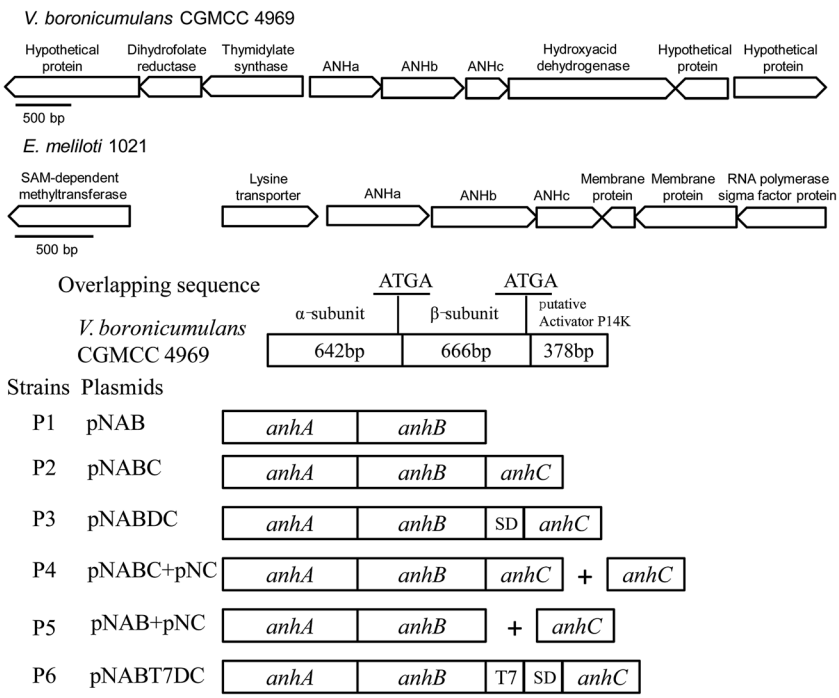

Fig. 1 Construction of recombinant plasmids and over-expression strains containing different components of the CGMCC 4969 ANHase gene cluster and the compositions of the ANHase gene clusters in *V. boronicumulans* CGMCC 4969 and *E. meliloti* CGMCC 7333.

Table 2 Primers used in the construction of recombinant plasmids in this study[a]

Primer	Sequence (5′–3′)
P1-F	**ACAGCAAATGGGTCGCGGATCC**GAATTC ATGACCGGCCATGACCACTCCCAC
P1-R	**ATCTCAGTGGTGGTGGTGGTGGTG**CTCG AGTGCCGCGGGCTCCAGGTAGCTT
P2-F	**ACAGCAAATGGGTCGCGGATCC**GAATTCA TGACCGGCCATGACCACTCCCAC
P2-R	**ATCTCAGTGGTGGTGGTGGTGGTG**CTCGA GGCCCGGAAAGTCTTCGCCGC
P3-F1	**ACAGCAAATGGGTCGCGGATCC**GAATTCATG ACCGGCCATGACCACTCC
P3-R1	**ATGGTATATCTCCTTCTTAAAGTTCT**ATGCCG CGGGCTCCAGGTAG
P3-F2	**AGAACTTTAAGAAGGAGATATACCAT**ATGAAG GCGAACGACATGCCG
P3-R2	**ATCTCAGTGGTGGTGGTGGTGGTG**CTCGAG GCCCGGAAAGTCTTCGCCGC
P4-F	**ACAGCAAATGGGTCGCGGATCC**GAATTCAT GAAGGCGAACGACATGCCG
P4-R	**ATCTCAGTGGTGGTGGTGGTGGTG**CTCGAG CTAGCCCGGAAAGTCTTCGCC
P6-F1	**ACAGCAAATGGGTCGCGGATCC**GAATTCAT GACCGGCCATGACCACTCCCAC
P6-R1	**GTGAGTCGTATTAATTTCGCGGGATCTA**TGC CGCGGGCTCCAGGTAG
P6-F2	TAGATCCCGCGAAATTAATACGACTC
P6-R2	**ATCTCAGTGGTGGTGGTGGTGGTG**CTCGAG CTAGCCCGGAAAGTCTTCGC

[a] Underlined bases indicate the restriction enzyme sites of *Eco*RI (GAATTC) and *Xho*I (CTCGAG), respectively. Boldface bases indicate the homologous fragment used in the ligation between the target fragment and the expression vector.

structural α and β genes (*anhAB*) and *anhAB* with *anhC* (*anhABC*) were amplified by polymerase chain reaction (PCR) using primer pairs P1 (P1-F and P1-R) and P2 (P2-F and P2-R), which have a pET28a homologous base located before the corresponding restriction enzyme sites, *Eco*RI and *Xho*I. The PCR system was composed of 0.4 μL of genomic DNA template of CGMCC 4969 (100 ng μL^{-1}), 0.4 μL of each primer (20 mmol L^{-1}), 4 μL of PrimerSTAR buffer (Mg^{2+} plus, 5×), 0.2 μL of PrimerSTAR DNA polymerase (2.5 U μL^{-1}, Takara), 2 μL of dNTP (2.5 mmol L^{-1} each), and 12.6 μL of sterilized distilled water. The total volume of the reaction mixture was 20 μL. After an initial pre-denaturation for 5 min at 95 °C, the cycling conditions were as follows: denaturation for 50 s at 95 °C, annealing for 40 s at 60 °C, and extension for 2 min at 72 °C. A final 10 min extension step at 72 °C was performed after 29 cycles. The PCR product was analyzed using 1% agarose gel electrophoresis. The *anhAB* or *anhABC* fragment was ligated to the expression plasmid pET28a, which was performed according to the protocol of the ClonExpress II one step cloning kit (Vazyme Biotech, Nanjing, China). The recombinant plasmids pNAB and pNABC were verified using DNA sequencing by Springen Biotech (Nanjing, China).

To examine the influence of the enhanced expression of *anhC* on the ANHase activity for AAP hydration, the efficient Shine–Dalgarno (SD) sequence of the T7 phage from the pET expression system was introduced to the 5′-terminus of *anhC* by overlap extension PCR. First, *anhAB* was amplified by PCR using primers P3-F1 and P3-R1; meanwhile, *anhC* was amplified using primers P3-F2 and P3-R2. The SD sequence was added to the downstream primer P3-R1 and upstream primer P3-F2 as a homologous fragment. Finally, the two DNA fragments were combined using the outer primers P3-F1 and P3-R1, and the resulting fragment was named *anhABDC*. In addition, the strong T7 promoter was also introduced to the 5′-terminus of *anhC* according to the method referred to above, except that the primers P6-F1, P6-R1, P6-F2, and P6-R2 were used and the homologous fragment was the T7 promoter. The resulting DNA fragment was named *anhABT7DC*. The fragments *anhABDC* and *anhABT7DC* were inserted into pET28a according to the above-mentioned protocol, and the obtained plasmids were named pNABDC and pNABT7DC, respectively.

We also constructed a double-plasmids expression system employing plasmids pET28a and pET21a. The *anhC* fragment was independently inserted into the expression vector pET21a using primers P4-F and P4-R to obtain the plasmid pNC, and then the two plasmids were co-transformed in the host *E. coli* Rosetta (DE3).

2.7 Expression and purification of recombinant ANHase in *E. coli* Rosetta (DE3) pLysS

Transformation of the recombinant plasmids to the competent cells of *E. coli* Rosetta (DE3) pLysS and over-expression of the recombinant ANHase were conducted according to the method described in our previous report.[25] To investigate degradation by the *E. coli* resting cells containing different *anh*s, the over-expressed strains were washed twice with 0.2 mol L^{-1} sodium phosphate buffer (pH 7.5) and then resuspended in the same buffer containing 500 mg L^{-1} AAP, and the optical density of the cells at 600 nm was adjusted to 3. After transformation for 10 min at 30 °C, each sample was analyzed by HPLC. To further explore the expression of the different recombinant *anh*s, equal amounts of cell pellets were suspended in a 1 mL volume of 0.2 mol L^{-1} phosphate buffer and disrupted by sonication (10 s) for 3 min at ice temperature. The soluble and insoluble fractions were separated by centrifugation at 12 000 *g* for 10 min at 4 °C prior to recombinant protein detection. The purification of the ANHase by His-tag affinity chromatography was conducted according to the protocol of the manufacturer of the chromatography resin (Novagen, Inc.). Western blot and sodium dodecyl sulfate polyacrylamide gel electrophoresis (SDS-PAGE) were carried out according to the method described by Yang *et al.*[27]

2.8 Enzyme assay

The standard assay was carried out by mixing 500 mg L^{-1} AAP and an appropriate amount of enzyme in 0.2 mol L^{-1} sodium phosphate buffer (pH 7.5). The reaction mixtures with total volumes of 1 mL were incubated for 10 min at 37 °C and quenched by addition of 10% (v/v) 2 mol L^{-1} hydrochloric acid. Then, the samples were centrifuged at 12 000 *g* for 10 min and

the supernatants were analyzed by HPLC. The ANHase activity toward aliphatic nitrile compounds was assessed by quantifying the amount of ammonia released during the reaction according to the methods reported by Okamoto and Eltis.[28] The ANHase reaction was coupled with an aliphatic amidase from CGMCC 4969 (GenBank accession number AFP67897), which was heterologously produced in *E. coli* Rosetta with a His-tag at the N terminus and purified using a Ni-NTA resin. One unit (U) of ANHase activity was defined as the amount of enzyme that catalyzed the formation of 1 μmol of product in 1 min.

2.9 Characteristics of the purified recombinant ANHase

The optimal pH was determined by adding AAP to different 0.2 mol L^{-1} sodium citrate (pH 4–6), phosphate (pH 6–8), and Tris–HCl (pH 8–10) buffers to a final concentration of 500 mg L^{-1}. For pH stability, the enzyme was incubated at 4 °C for 12 h in buffers at different pH values and the residual ANHase activity was determined using the method previously described. Reaction mixtures at temperatures from 20 to 60 °C at the optimal pH were used to determine the optimal temperature of ANHase activity. For thermal stability, the enzyme was pre-incubated at different temperatures for 1 h, and the non-heated ANHase was used as the control and its activity was defined as 100%.

The effects of metal ions on ANHase activity were determined by individually adding $CoCl_2$, $CaCl_2$, $CuCl_2$, $FeCl_2$, $MnCl_2$, $ZnCl_2$, $MgCl_2$, and $AgNO_3$ at a final concentration of 1 mmol L^{-1}. Acetone, ethanol, ethyl acetate, dichloromethane, hexane, methanol, and isopropanol (at a volume ratio of 2%) were individually added to the standard reaction mixture to test the effects of organic reagents on ANHase activity. Enzyme activity without any additives was used as the control and its activity for AAP was defined as 100%.

To broaden the application spectrum of the CGMCC 4969 ANHase, THI, IAN, 2-cyanopyridine, 3-cyanopyridine, benzonitrile, and the aliphatic nitriles acetonitrile, butyronitrile, isobutyronitrile, succinonitrile, and hexanedinitrile were used as substrates. Each reaction was conducted in a 1 mL mixture containing 2 mmol L^{-1} substrate and an appropriate amount of enzyme.

The kinetic parameters for the activity of the ANHase toward AAP were calculated by determining the initial velocity of AAP hydration in the range of from 0.2 to 5 mmol L^{-1} AAP. The maximal hydration rate (V_{max}) and apparent Michaelis–Menten constant (K_m) were deduced from Lineweaver–Burk plots.

3. Results and discussion

3.1 Biodegradation of AAP by *V. boronicumulans* CGMCC 4969 in the culture medium and surface water

The ability of the resting cells of *V. boronicumulans* CGMCC 4969 to degrade AAP was primarily examined in phosphate buffer. As shown in Fig. 2A–C, after transformation for 48 h, a new polar peak at retention time of 3.91 min appeared, whereas no comparable peak was observed upon analysis of controls containing the bacterium or AAP alone, and 41.6% of AAP was degraded (Fig. 2D). LC-MS analysis indicated that the metabolite displayed a protonated parent ion (M + H) at *m/z* 241, a sodiated adduct (M + Na) at *m/z* 263, a fragment ion (M − CHON) at *m/z* 198, a fragment ion (M − C_3H_2NO) at *m/z* 157, a fragment ion (M − $C_4H_8N_3O$) at *m/z* 126, and a fragment ion (M − $C_6H_6N_2Cl$) at *m/z* 99. The ^{13}C NMR data of the purified metabolite were as follows: 165.4, 160.8, 149.5, 149.4, 139.5, 133.7, 124.5, 49.3, 36.1, and 16.4; The ^{1}H NMR data of the purified metabolite were as follows: 8.33 (s, 1H), 7.76 (d, 1H, J = 7.2 Hz), 7.48 (d, 1H, J = 8.4), 6.29, 6.13 (b, 2H), 4.61 (s, 2H), 2.91 (s, 3H), and 2.12 (s, 3H). The mass and NMR data of the metabolite formed by AAP degradation by *V. boronicumulans* CGMCC 4969 were found to be identical to those reported for (*E*)-N^2-carbamoyl-N^1-[(6-chloro-3-pridyl)methyl]-N^1-methyl-acetamidine (usually denoted as IM-1-2),[16] and therefore, the metabolite was identified as IM-1-2.

As shown in Fig. 2E, after inoculating *V. boronicumulans* CGMCC 4969 in surface water and incubating for 5 days, the AAP content was reduced from 1.96 mg L^{-1} to 1.28 mg L^{-1} and the degradation rate was 34.7%. AAP degradation fitted first-order dissipation kinetics (R = 0.99) with a half-life of 182 h. In contrast, AAP was barely degraded in control water without bacterial inoculation. We previously isolated an *E. meliloti* CGMCC 7333, which could degrade 65.1% of 500 mg L^{-1} AAP in 96 h with a half-life of 63 h.[16] However, this strain showed weak AAP degradation in surface water samples (data not shown). *E. meliloti* (formerly *Sinorhizobium meliloti*) is a symbiotic nitrogen-fixing bacterium, and is usually limited by application of microbes–plants combined remediation. In contrast, *Variovorax* spp. are common inhabitants of soil and water environments, and therefore *V. boronicumulans* CGMCC 4969 showed potential ability to degrade AAP in water.

The metabolism of AAP in plants, animals, and soils involves three pathways: *N*-demethylation of AAP to IM-2-1; oxidative cleavage of the cyanoimine group to form IM-1-3, and subsequent *N*-deacetylation to form IM-1-4; hydration of AAP to the *N*-carbamoylimine derivative (IM-1-2), which is spontaneously hydrolyzed to IM-1-4.[29] As shown in Fig. 2D, 0.44 mg L^{-1} IM-1-2 was formed and the molar conversion rate (the amount of IM-1-2 formed divided by the amount of AAP reduced) was 66.2%, indicating that AAP hydration to IM-1-2 is the major metabolic pathway in the degradation of AAP in surface water by *V. boronicumulans* CGMCC 4969. This metabolic pathway is different from that of biodegradation of AAP by *Micrococcus luteus* SC 1204, which occurs *via* the formation of the benzothiazole 2-(2-hydroxyethylthio) metabolite.[30]

3.2 Bioinformatics analysis of the *V. boronicumulans* CGMCC 4969 ANHase gene cluster

A typical strain of the genus *Variovorax*, *Variovorax paradoxus* S110, has two ANHase gene clusters: one involving three genes (Vapar_1665, Vapar_1666, and Vapar_1667) and another with two genes (Vapar_2111 and Vapar_2112). In contrast, *V. paradoxus* EPS has only one ANHase gene cluster with three genes (Varpa_1815, Varpa_1816, and Varpa_1817). In the present study, genomic DNA sequencing analysis indicated that there is

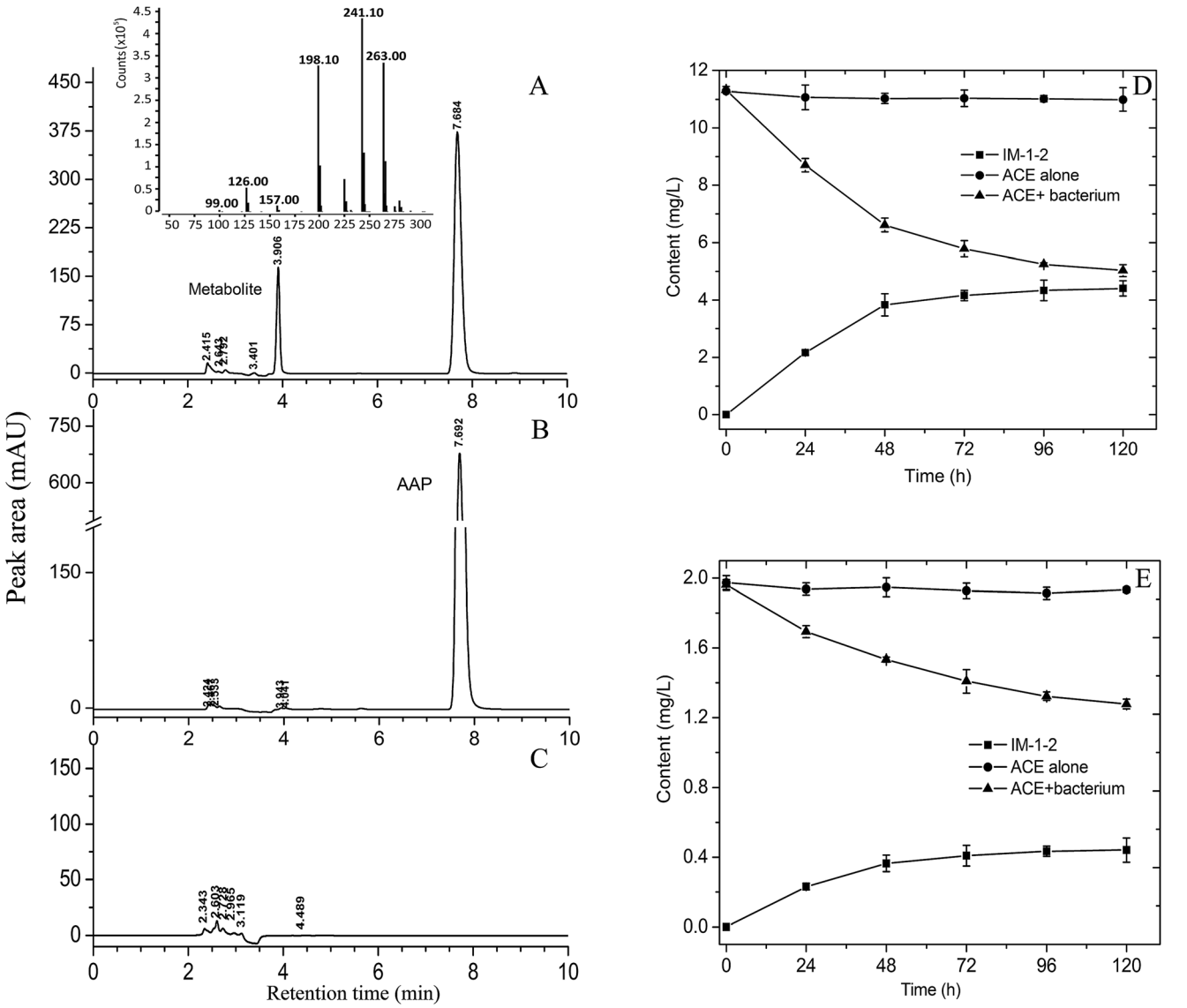

Fig. 2 HPLC and LC-MS analyses and the time course of AAP biodegradation by resting cells of *V. boronicumulans* CGMCC 4969. (A) Transformation broth with inoculation of bacterium and addition of AAP; (B) transformation broth with AAP alone; (C), transformation broth with inoculation of bacterium alone. (D) Resting cells with inoculation of bacterium (2.5×10^9 cell per mL) and AAP (12 mg L^{-1}) in 50 mmol L^{-1} phosphate buffer. (E) Resting cells with inoculation of bacterium (1.28×10^8 cell per mL) and AAP (2 mg L^{-1}) in water samples.

only one ANHase coding gene cluster in the genome of *V. boronicumulans* CGMCC 4969, which is composed of three genes (Fig. 1), a 642 bp α-subunit coding gene (named *anhA*), a 666 bp β-subunit coding gene (named *anhB*), and a 378 bp hypothetical protein coding gene (named *anhC*) (GenBank accession number KC460345). During the microbial metabolism of nitrile compounds, ANHase converts the nitrile compound to an amide intermediate and an amidase subsequently converts the amide product to an acid metabolite, and therefore the amidase coding gene is usually located at a site close to the ANHase gene. For example, in the low molecular mass ANHase gene cluster of *Rhodococcus rhodochrous* J1, an amidase encoding gene *amdA* was located 1.9 kb downstream of the ANHase coding gene *nhlBA*,[31] and an amidase gene was found to be located upstream of the ANHase coding gene in *Pseudomonas chlororaphis* B23.[32]

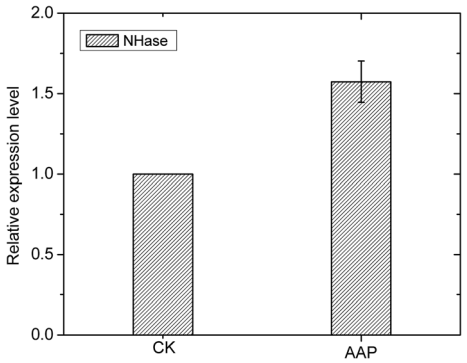

Fig. 3 mRNA expression levels of the ANHase gene of *V. boronicumulans* CGMCC 4969. CK, control; AAP, addition of AAP to the culture medium. Error bars represent the standard deviations of three replicates.

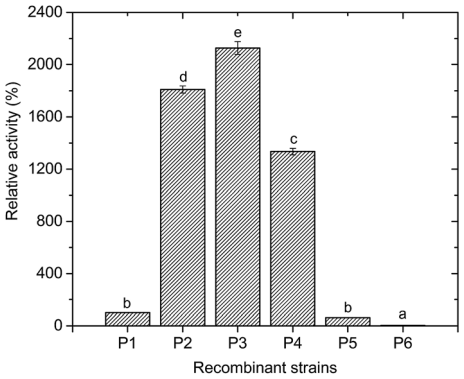

Fig. 4 Activity analysis of recombinant *E. coli* Rosetta strains containing different components of the CGMCC 4969 ANHase gene cluster. The ANHase activity was assayed under the standard assay conditions with AAP as the substrate. Different letters (a–e) above the columns represent significant differences at $p \leq 0.05$ according to the Duncan test.

However, as shown in Fig. 2, there is no adjacent amidase gene in the ANHase gene cluster of CGMCC 4969. The genes upstream, *anhA*, code the enzymes related to folic acid synthesis and the genes downstream, *anhC*, code an oxidoreductase and an uncharacterized membrane protein (Fig. 1). The same results, namely that no amidase coding gene was located near the ANHase gene cluster, were observed in another AAP-degrading bacterium, *Ensifer meliloti* 1021 (Fig. 1). Both CGMCC 4969 and CGMCC 7333 have the same rank of *anhA* (α-subunit), *anhB* (β-subunit), and *anhC* (accessory protein) and have the same overlapping sequence "ATGA" between *anhA* and *anhB*. However, the overlapping sequence "ATGA" also appeared between *anhB* and *anhC* of CGMCC 4969, whereas a 14 bp overlapping sequence "TTGAACCCGCATAG" appeared between *anhB* and *anhC* of CGMCC 7333.

Protein blast analysis indicated that ANHc exhibits the maximum identity of 95% with the ANHase accessory protein of *Variovorax* sp. Root473 (GenBank accession number AGI48675), and about 75% identity with the ANHase accessory protein of *Bradyrhizobium elkanii* (GenBank accession number WP_028165648). However, CGMCC 4969 ANHc only has 41.7% identity with the ANHase accessory protein of *E. meliloti* CGMCC 7333 (GenBank accession number KF601244), a nitrogen-fixing bacterium shown to be capable of degrading AAP.[16]

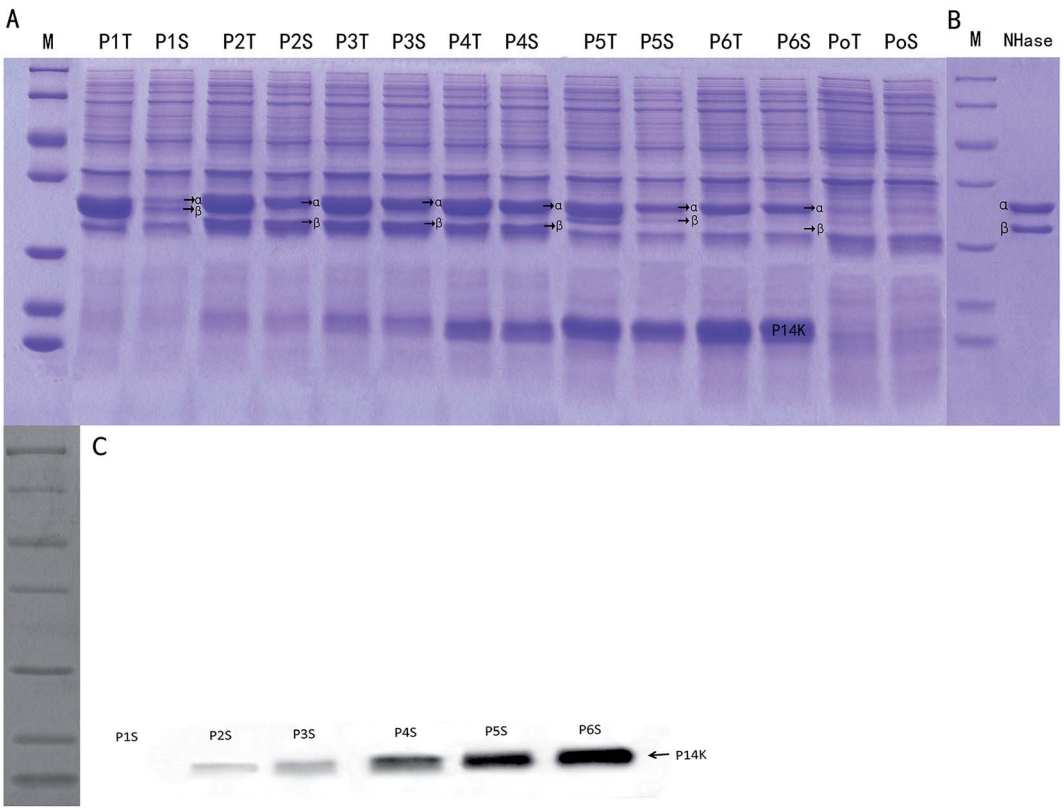

Fig. 5 SDS-PAGE and western blotting analyses of different components of the CGMCC 4969 ANHase gene cluster over-expressed in *E. coli* Rosetta and the purified recombinant ANHase. (A) SDS-PAGE of different components of the CGMCC 4969 ANHase gene cluster; lanes P1T, P2T, P3T, P4T, P5T, P6T represent the total protein of *E. coli* Rosetta (DE3) P1–P6, and lanes P1S, P2S, P3S, P4S, P5S, P6S represent the soluble protein of *E. coli* Rosetta (DE3) P1–P6, respectively; lanes PoT and PoS represent the control *E. coli* Rosetta (DE3) containing the pET28a plasmid alone; lane M represents standard protein markers (116.0, 66.2, 45.0, 35.0, 25.0, 18.4, and 14.4 kDa from top to bottom); (B) purified recombinant ANHase from strain P3; (C) western blotting analysis of the expression levels of the activator. A 6× histidine tag was added to the N-terminus of the α-subunit and C-terminus of the β-subunit of strains P1, P5 and the N-terminus of the α-subunit and C-terminus of the activator for strains P2, P3, P4, P6.

3.3 Transcript analysis of the ANHase gene cluster in *V. boronicumulans* CGMCC 4969

To further analyze the influence of AAP on the expression of the ANHase gene cluster, MSM medium containing AAP as the only nitrogen source was used to cultivate *V. boronicumulans* CGMCC 4969 cells. As shown in Fig. 3, AAP treatment significantly upregulated the expression of the ANHase gene by 1.6-fold, when compared with that in the control, suggesting the participation of *V. boronicumulans* CGMCC 4969 cells in the degradation of AAP.

3.4 Effect of co-expression of *anhC* with *anhAB* and the effect of the expression level of *anhC* on ANHase activity for AAP hydration

The control *E. coli*-pET28a that did not harbor the ANHase gene cluster did not convert AAP to IMI-1-2 (ESI Fig. S1†), while *E. coli*-pET28a-*anhAB* (strain P1) could make this conversion, which indicates that CGMCC 4969 ANHase was responsible for AAP degradation to IM-1-2. As shown in Fig. 4, *E. coli*-pET28a-*anhABC* (strain P2) showed an 18-fold higher ANHase activity than strain P1. SDS-PAGE analysis (Fig. 5A) indicated that the P1 ANHase was mainly expressed with the inclusion body as compared to the total protein fraction (lane P1T) with the soluble protein fraction (lane P1S). In lane P2T, the over-expressed ANHc with molecular weight of 14 kDa can be clearly observed. The total protein expression level of ANHa was not higher, whereas the soluble fraction (lane P2S) was significantly higher, when compared with P1. These results prove that ANHc plays an important role in the maturation of CGMCC 4969 ANHase by improving its solubility and therefore increasing its enzymatic activity.

The SD fragment, the RNA polymerase binding site, was introduced between *anhB* and *anhC*, and the constructed plasmid pNABDC was over-expressed in *E. coli* (named strain P3). As shown in Fig. 5, lanes P3T and P3S, the expression level of the activator protein ANHc was further increased compared to P2 as shown by SDS-PAGE (Fig. 5A) and western blotting analysis (Fig. 5C). The ANHase activity of P3 for AAP hydration was the highest and was 21-fold higher than that of P1 and 1.2-fold higher than that of P2. Increasing expression levels of ANHc coincided with promotion of ANHase activity. Therefore, we further engineered the independent over-expression of plasmid pNABT7DC, containing the T7 promoter sequence before the SD sequence, and plasmid pNC with the insertion of only *anhC* into pET21a. The pNC plasmid was co-expressed in *E. coli* with pNAB or pNABC. As shown in Fig. 5A, the strains P4, P5, and P6 are associated with gradually rising amounts of ANHc (lanes P4S, P5S, and P6S), and their expression levels were higher than those of P3 according to western blotting analysis (Fig. 5C). However, on the contrary, the ANHase activities of P4, P5, and P6 for AAP hydration were lower than that of strain P3 (Fig. 4). Strains P5 and P6 exhibited even lower ANHase activity than strain P1 without co-expression of ANHc. Comparing the ANHase expression of P5 with P1, the amount of ANHa in P5 (lane 5S) was higher than that in P1, whereas the amount of ANHb in P5 was lower than that in P1. Because the active ANHases exist as α2β2 tetramers and bind one metal atom per αβ unit, the reduced amount of ANHb in P5 decreased its ANHase activity to 62% of the activity of P1. Strain P6 exhibited

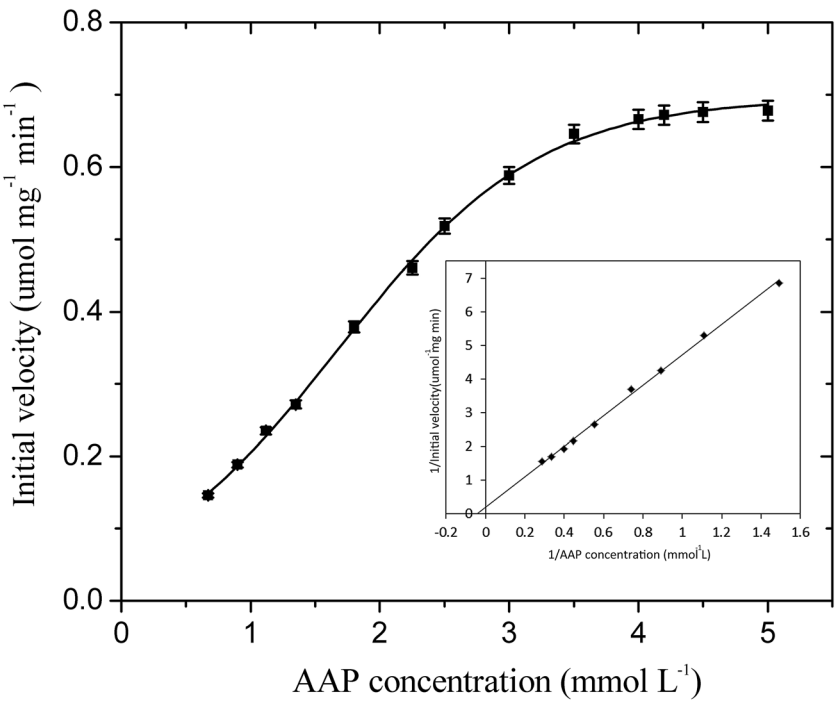

Fig. 6 The kinetic constants of CGMCC 4969 ANHase for the degradation of AAP. The kinetic parameters of the ANHase toward AAP were determined over a range of substrate concentrations (0.2–5 mmol L^{-1}) under standard assay conditions.

Table 3 Substrate specificities of the purified CGMCC 4969 ANHase[a]

Substrate	Relative activity ± standard deviation (%)
ACE	100 ± 1.61
THI	230.16 ± 4.24
IAN	1501.19 ± 39.62
2-Cyanopyridine	5068.10 ± 45.77
3-Cyanopyridine	7144.42 ± 110.42
Benzonitrile	5216.56 ± 72.81
Acetonitrile	35.03 ± 1.72
Butyronitrile	19.35 ± 0.71
Isobutyronitrile	3.82 ± 0.12
Succinonitrile	25.99 ± 2.03
Hexanedinitrile	1.81 ± 0.22

[a] ANHase activity was determined under standard assay conditions. The specific activity of AAP (0.67 U mg^{-1}) was taken as 100%.

the highest expression level of ANHc, whereas the expression of ANHb was hardly observed in lane 6S, and HPLC analysis indicated that P6 had very little ANHase activity for AAP hydration (Fig. 4).

We also studied the effect of co-expression of the *E. meliloti* CGMCC 7333 *anhC* with *anhAB* on the ANHase activity for AAP hydration. The results indicate that strain P2 of CGMCC 7333 only had 4-fold higher ANHase activity than strain P1 (data not shown). In the present study, strain P2 with over-expressed CGMCC 4969 *anhABC* had 18-fold higher ANHase activity than strain P1 with over-expressed *anhAB*. We speculate that the poor enhancement of ANHase activity by CGMCC 7333 ANHc was due to the longer overlapping sequence between CGMCC 7333 *anhB* and *anhC* compared to that of CGMCC 4969. In strain P5, although the expression level of ANHc was much higher than in P2, the enhanced ANHc expression did not increase the ANHase activity, which was 30-fold lower than the activity of P2 and 38% lower than that of P1. As compared with strain P1, harboring pNAB, the independent plasmid pNC (pET21a-*anhC*) was further introduced to P5. The independent over-expression of ANHc displayed an inhibitory effect on the level of the soluble protein fraction of ANHb but a promoting effect on that of ANHa (Fig. 5 lane 5S). These reverse effects of ANHc on the expressions of ANHa and ANHb have not been reported in previous studies and the mechanism needs further exploration.

3.5 Biochemical properties of the recombinant ANHase

3.5.1 The kinetic parameters of purified ANHase. Recombinant ANHase in strain P3 was expressed as a His-tag-labelled protein at the N-terminus of the ANHase α-subunit and C-terminus of the activator ANHc. Ni-NTA affinity chromatography was used to purify the recombinant CGMCC 4969 ANHase. SDS-PAGE showed two definite protein bands for the α-subunit and β-subunit (Fig. 5B). The purified ANHase was used to determine its biochemical properties.

Although the kinetic parameters of the ANHase toward various nitriles have been extensively reported,[33] parameters for the neonicotinoid insecticide AAP degradation have rarely been cited. As shown in Fig. 6, the K_m and V_{max} values of the ANHase for AAP were 21.83 mmol L^{-1} and 4.84 μmol min^{-1} mg^{-1}, respectively.

3.5.2 Substrate specificity. As shown in Table 3, ANHase can hydrate another cyano-containing neonicotinoid, THI, and its activity is 2.3-fold higher than for the AAP substrate. ANHase also transformed various nitrile compounds, including the aromatic benzonitrile, IAN, N-heterocyclic 3-cyanopyridine, 2-cyanopyridine, and the aliphatic acetonitriles, butyronitrile,

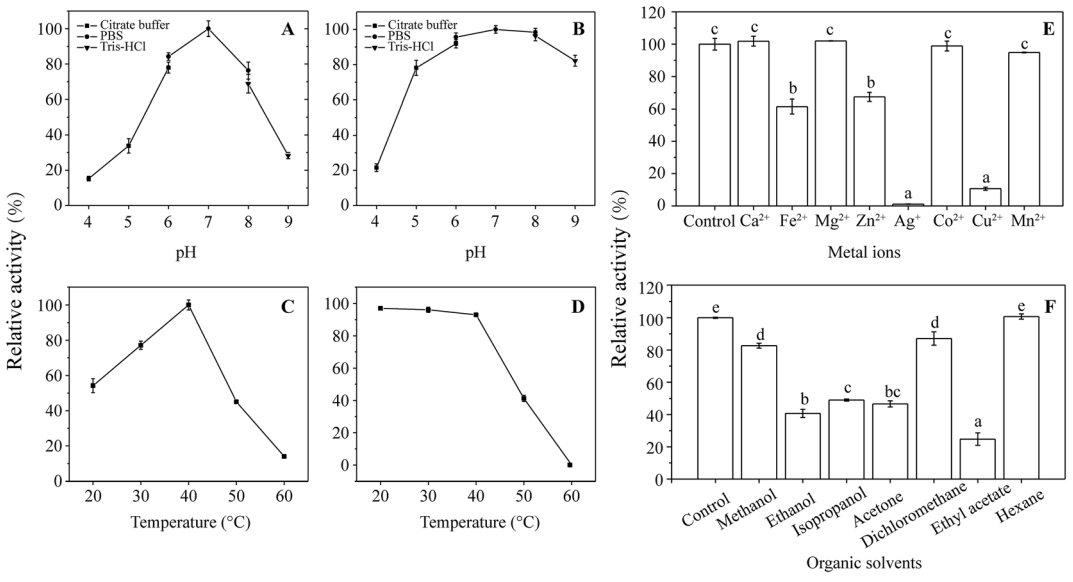

Fig. 7 Enzymatic characterization of the purified recombinant ANHase. (A) Effects of pH on the activity of ANHase; (B) effects of pH on the stability of ANHase; (C) effects of temperature on the activity of ANHase; (D) effects of temperature on the stability of ANHase; (E) effects of metal ions on the activity of ANHase; (F) effects of organic solvents on the stability of ANHase. Different letters (a–e) above the columns represent significant differences at $p \leq 0.05$ according to the Duncan test.

isobutyronitrile, succinonitrile, and hexanedinitrile. In contrast, *Bacillus pallidus* Dac521 ANHase only hydrolyzed aliphatic nitriles but not dinitriles nor any of the cyclic, aromatic nitriles.[34] Similarly, *Pseudomonas chlororaphis* B23 and *Bacillus* RAPc8 ANHase showed no selectivity for aromatic nitriles, such as benzonitrile.[35,36] Among the substrates investigated, 3-cyanopyridine was the substrate associated with the highest ANHase activity of 48.1 U mg^{-1}, whereas 2-cyanopyridine, different only in the position of the substituent cyano group, showed 29% lower activity than 3-cyanopyridine, which may be due to steric effects in that the *meta* derivatives were better substrates than the *ortho* derivatives. For the aliphatic nitriles, ANHase showed a preference for the short chain of acetonitrile compared to the long chain of butyronitrile, as well as for the dinitriles succinonitrile and hexanedinitrile.

3.5.3 Effects of temperature and pH on the activity of ANHase for AAP hydration. As shown in Fig. 7A, the optimal pH of ANHase for AAP hydration was 7.0, which is in accordance with ANHases from *Agrobacterium tumefaciens* d3, *Arthrobacter* sp. J1, and *Bacillus* sp. RAPc8.[37] Furthermore, ANHase had a broad spectrum of pH stability, retaining over 78% activity when the pH ranged from 5.0 to 9.0 (Fig. 7B). The maximum ANHase activity for AAP hydration was observed at a temperature of 40 °C (Fig. 7C), which was similar to the mesophilic ANHase from *R. rhodochrous* J1.[38] When the incubation temperature reached 50 °C, more than 50% of the activity was lost (Fig. 7D).

3.5.4 Effects of metal ions and organic solvents on ANHase activity for AAP hydration. As shown in Fig. 7E, Ca, Mg, and Mn ions had little effect on the ANHase activity, whereas Cu and Ag ions exhibited more than 80% inhibitory effect on ANHase activity. Inhibition by Ag and Cu ions was also found for the ANHases from *Bacillus* sp. RAPc8 and *Pseudomonas chlororaphis* B23,[35,36] but in *Arthrobacter* sp. J-1 and *R. rhodochrous* PA-34,[39,40] Cu inhibition was not seen.

As shown in Fig. 7F, ethanol, isopropanol, acetone, and ethyl acetate inhibited ANHase activity by more than 50% compared with the control. Methanol and dichloromethane retained >80% activity when 2% (v/v) organic solvent was added to the reaction system. In contrast, hexane, with a log *P* value of 3.5, displayed no inhibition of ANHase activity, which may because biocatalysis is likely to occur with solvents of higher log *P* values and inhibition in the presence of hydrophilic solvents (log $P < 2.0$).[41]

4. Conclusions

In the present study, we found the neonicotinoid insecticide AAP was degraded to IM-1-2 in surface water by *V. boronicumulans* CGMCC 4969, and this was mediated by ANHase. Co-expression of downstream *anhC* apparently improved ANHase activity 21-fold, but independent over-expression of *anhC* inhibited the expression of the β-subunit, which resulted in decreasing ANHase activity. CGMCC 4969 ANHase is a versatile ANHase that is capable of hydrating aromatic, N-heterocyclic, and aliphatic nitriles.

Acknowledgements

This research was financed by the Priority Academic Program Development (PAPD) of Jiangsu Higher Education Institutions, the National Science Foundation of China (grant No. 31570104), and the Academic Natural Science Foundation of Jiangsu Province (grant No. 14KJA180004).

References

1 P. Jeschke, R. Nauen, M. Schindler and A. Elbert, *J. Agric. Food Chem.*, 2011, **59**, 2897–2908.
2 M. Tomizawa, D. L. Lee and J. E. Casida, *J. Agric. Food Chem.*, 2000, **48**, 6016–6024.
3 D. Goulson and D. Kleijn, *J. Appl. Ecol.*, 2013, **50**, 977–987.
4 C. A. Morrissey, P. Mineau, J. H. Devries, F. Sanchez-Bayo, M. Liess, M. C. Cavallaro and K. Liber, *Environ. Int.*, 2015, **74**, 291–303.
5 D. Gibbons, C. Morrissey and P. Mineau, *Environ. Sci. Pollut. Res. Int.*, 2015, **22**, 103–118.
6 L. W. Pisa, V. Amaral-Rogers, L. P. Belzunces, J. M. Bonmatin, C. A. Downs, D. Goulson, D. P. Kreutzweiser, C. Krupke, M. Liess, M. McField, C. A. Morrissey, D. A. Noome, J. Settele, N. Simon-Delso, J. D. Stark, J. P. Van der Sluijs, H. Van Dyck and M. Wiemers, *Environ. Sci. Pollut. Res. Int.*, 2015, **22**, 68–102.
7 C. Leandro, V. Souza, E. F. Dores and M. L. Ribeiro, *J. Braz. Chem. Soc.*, 2008, **19**, 1111–1117.
8 J. Anderson, C. Dubetz and V. Palace, *Sci. Total Environ.*, 2015, **505**, 409–422.
9 X. L. Wu, L. Meng, Y. Wu, Y.-Y. Luk, Y. Ma and Y. Du, *J. Braz. Chem. Soc.*, 2015, **26**, 131–139.
10 J. Struger, J. Grabuski, S. Cagampan, E. Sverko, D. McGoldrick and C. H. Marvin, *Chemosphere*, 2017, **169**, 516–523.
11 I. Carra, J. A. Sánchez Pérez, S. Malato, O. Autin, B. Jefferson and P. Jarvis, *J. Chem. Technol. Biotechnol.*, 2016, **91**, 72–81.
12 V. Guzsvány, J. Csanádi and F. Gaál, *Acta Chim. Slov.*, 2006, **53**, 52.
13 A. Khan, M. Haque, N. A. Mir, M. Muneer and C. Boxall, *Desalination*, 2010, **261**, 169–174.
14 E. E. Mitsika, C. Christophoridis and K. Fytianos, *Chemosphere*, 2013, **93**, 1818–1825.
15 Y. J. Dai, W. W. Ji, T. Chen, W. J. Zhang, Z. H. Liu, F. Ge and S. Yuan, *J. Agric. Food Chem.*, 2010, **58**, 2419–2425.
16 L. Y. Zhou, L. J. Zhang, S. L. Sun, F. Ge, S. Y. Mao, Y. Ma, Z. H. Liu, Y. J. Dai and S. Yuan, *J. Agric. Food Chem.*, 2014, **62**, 9957–9964.
17 H. Tang, J. Li, H. Hu and P. Xu, *Process Biochem.*, 2012, **47**, 1820–1825.
18 G. Wang, W. Yue, Y. Liu, F. Li, M. Xiong and H. Zhang, *Bioresour. Technol.*, 2013, **138**, 359–368.
19 H. Yang, X. Wang, J. Zheng, G. Wang, Q. Hong, S. Li, R. Li and J. Jiang, *Int. Biodeterior. Biodegrad.*, 2013, **85**, 95–102.
20 S. S. Phugare and J. P. Jadhav, *Clean: Soil, Air, Water*, 2015, **43**, 296–304.

21 T. Chen, Y. J. Dai, J. F. Ding, S. Yuan and J. P. Ni, *Biodegradation*, 2008, **19**, 651–658.
22 Z. H. Liu, Y. M. Cao, Q. W. Zhou, K. Guo, F. Ge, J. Y. Hou, S. Y. Hu, S. Yuan and Y. J. Dai, *Biodegradation*, 2013, **24**, 855–864.
23 H. J. Zhang, Q. W. Zhou, G. C. Zhou, Y. M. Cao, Y. J. Dai, W. W. Ji, G. D. Shang and S. Yuan, *J. Agric. Food Chem.*, 2012, **60**, 153–159.
24 M. Owsianiak, A. Dechesne, P. J. Binning, J. C. Chambon, S. R. Sørensen and B. F. Smets, *Environ. Sci. Technol.*, 2010, **44**, 7622–7627.
25 F. Ge, L.-Y. Zhou, Y. Wang, Y. Ma, S. Zhai, Z.-H. Liu, Y.-J. Dai and S. Yuan, *Int. Biodeterior. Biodegrad.*, 2014, **93**, 10–17.
26 S.-L. Sun, T.-Q. Lu, W.-L. Yang, J.-J. Guo, X. Rui, S.-Y. Mao, L.-Y. Zhou and Y.-J. Dai, *RSC Adv.*, 2016, **6**, 15501–15508.
27 Y. Yang, T. Chen, P. Ma, G. Shang, Y. Dai and S. Yuan, *Biodegradation*, 2010, **21**, 593–602.
28 S. Okamoto and L. D. Eltis, *Mol. Microbiol.*, 2007, **65**, 828–838.
29 J. E. Casida, *J. Agric. Food Chem.*, 2011, **59**, 2923–2931.
30 T. Kanjilal, C. Bhattacharjee and S. Datta, *J. Water Process Eng.*, 2015, **6**, 21–31.
31 H. Komeda, M. Kobayashi and S. Shimizu, *J. Biol. Chem.*, 1996, **271**, 15796–15802.
32 M. Nishiyama, S. Horinouchi, M. Kobayashi, T. Nagasawa, H. Yamada and T. Beppu, *J. Bacteriol.*, 1991, **173**, 2465–2472.
33 Y.-S. Feng, P.-C. Chen, F.-S. Wen, W.-Y. Hsiao and C.-M. Lee, *Process Biochem.*, 2008, **43**, 1391–1397.
34 R. A. Cramp and D. A. Cowan, *Biochim. Biophys. Acta, Protein Struct. Mol. Enzymol.*, 1999, **1431**, 249–260.
35 T. Nagasawa, H. Nanba, K. Ryuno, K. Takeuchi and H. Yamada, *Eur. J. Biochem.*, 1987, **162**, 691–698.
36 R. A. Pereira, D. Graham, F. A. Rainey and D. A. Cowan, *Extremophiles*, 1998, **2**, 347–357.
37 A. Banerjee, R. Sharma and U. C. Banerjee, *Appl. Microbiol. Biotechnol.*, 2002, **60**, 33–44.
38 M. Odaka, K. Fujii, M. Hoshino, T. Noguchi, M. Tsujimura, S. Nagashima, M. Yohda, T. Nagamune, Y. Inoue and I. Endo, *J. Am. Chem. Soc.*, 1997, **119**, 3785–3791.
39 Y. Asano, K. Fujishiro, Y. Tani and H. Yamada, *Agric. Biol. Chem.*, 2014, **46**, 1165–1174.
40 S. Prasad, J. Raj and T. C. Bhalla, *Indian J. Microbiol.*, 2009, **49**, 237–242.
41 C. Laane, S. Boeren, K. Vos and C. Veeger, *Biotechnol. Bioeng.*, 1987, **30**, 81–87.